Stable cerium isotopes as a tracer of oxidation reactions

P. Bonnand[1,2*], M. Boyet[1], C. Bosq[1]

OPEN ACCESS

Abstract

https://doi.org/10.7185/geochemlet.2340
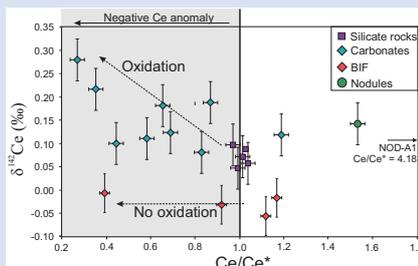
Redox conditions in past oceans have attracted significant interest and many proxies have been used to probe redox changes through time. For example, the redox dependent behaviour of Ce, resulting in negative or positive elemental Ce anomalies, has been widely used. More recently, mass dependent Ce isotopic variations have been proposed as a powerful tool to study Ce oxidation in natural environments. In this study, we demonstrate, for the first time, that Ce isotopes are fractionated during oxidation reaction, confirming the utility of Ce isotopes to study redox reactions. This result suggests that seawater Ce isotopic composition should be fractionated toward heavy values relative to the continental crust. Measured natural rock samples (carbonates, banded iron formations and Mn nodules) have variable Ce isotopic compositions, ranging from -0.055 ± 0.045 ‰ to $+0.280 \pm 0.045$ ‰. The relation between Ce elemental anomalies and Ce isotopic composition in carbonate rocks suggest that mass dependent Ce isotopes can be used to distinguish elemental anomalies produced by oxidation reactions from those produced by other processes. Coupled with La-Ce chronology, mass dependent Ce isotope analysis is a very powerful tool to study redox reactions in past oceans.

Introduction

The oxygenation of the atmosphere and oceans during Earth history has attracted significant interest in the scientific community. Over geological time, Earth's surface environments experienced dramatic evolution in prevailing redox conditions, as the concentration of atmospheric molecular oxygen (O_2) increased from levels of less than 1 part per million by volume before 2.45 Ga to 21 % by volume today. While the exact drivers continue to be debated, the accumulation of atmospheric oxygen ultimately became possible as the processes producing free oxygen (*e.g.*, hydrogen escape, carbon burial) exceeded the rate of oxygen consumption by different geological processes (*e.g.*, weathering, volcanic outgassing). Evidence from the ancient rock record suggests that atmospheric oxygenation occurred in steps, with a first rise of O_2 at 2.45–2.32 Ga and a second around 0.75–0.58 Ga (*e.g.*, Reinhard and Planavsky, 2022). The latter increase was a fundamental condition for the appearance of macroscopic animals. During the Phanerozoic, the oxygen concentration in the oceans also varied greatly, especially during great anoxic events of the Cenozoic (*e.g.*, Jenkyns, 2010). However, there remain significant unknowns regarding the timing and evolution of Earth surface oxygenation, especially for the first production of free oxygen by cyanobacteria sometime in the Archean and its initial accumulation in the atmosphere starting around 2.45 Ga.

Direct measurements of the chemical composition of the atmosphere in the past are impossible, and our understanding of the rise of oxygen in the atmosphere relies mainly on the sedimentary record and on redox proxies. The evidence for changes in redox state throughout geological times is multiple. The most decisive is probably the disappearance of mass independent fractionation of sulfur isotopes from the geological record (*e.g.*, Farquhar *et al.*, 2000). Moreover, several trace element proxies based on variations in metal concentrations and variations in their isotopic compositions have been developed to study the redox conditions in the ocean that can be directly correlated to the state of oxygenation in the atmosphere. For example, redox element enrichment, such as Mo, U and Cr, has been widely used to constrain the redox state of ancient oceans (*e.g.*, Brumsack, 2006). More recently, non-traditional stable isotopes have also been developed to help define the redox state of the ocean (*e.g.*, Eickmann *et al.*, 2018).

The redox behaviour of cerium and its unique ability to form Ce^{4+} ions among elements belonging to the rare Earth element (REE) have been used in the literature to study the redox conditions in modern and past environments (*e.g.*, Tostevin *et al.*, 2016). During magmatic processes, cerium is incompatible as other REE (affinity for the melt) and the main terrestrial reservoir for Ce is thus the continental crust. During oxidative weathering, Ce^{3+} is released into river waters and is later oxidised to Ce^{4+} (Elderfield *et al.*, 1990; German and Elderfield, 1990; Bau and Koschinsky, 2009). The chemical oxidation of cerium in seawater is believed to be mainly controlled by Mn and Fe cycling *via* Fe and Mn oxyhydroxides (Ohta and Kawabe, 2001; Bau *et al.*, 2014). Under oxidising conditions, Ce^{4+} is insoluble and readily absorbed onto particulates and Fe oxyhydroxides. Under reducing conditions, Ce^{3+} is soluble and behaves very similarly to its neighbours REE^{3+}, such as Pr and Nd. The redox dependent behaviour of cerium in seawater means that the residence time of Ce is short (less than 300 years) in oxic conditions.

1. Université Clermont Auvergne, CNRS, IRD, OPGC, Laboratoire Magmas et Volcans, 63000 Clermont-Ferrand, France
2. University Bretagne Occidentale-Brest, CNRS, IFREMER, Geo-Ocean, UMR 6538, IUEM, 29280 Plouzané, France
* Corresponding author (email: pierre.bonnand@univ-brest.fr)

Redox conditions in past oceans are classically investigated using Ce elemental anomalies. During the oxidation process, Mn-Fe oxyhydroxides are enriched in Ce relative to their neighbours and are characterised by positive Ce anomalies. Under oxidising conditions, cerium in seawater is thus depleted relative to its LREE neighbours (namely La, Pr and Nd), resulting in a negative Ce anomaly. On the other hand, under reducing conditions, Ce behaves similarly to other REE, resulting in no Ce anomaly. Although the Ce anomaly in natural environments has been largely used, the mechanisms responsible for the formation of elemental anomalies and the quantification of this process remain debated (e.g., Bau et al., 2014). For example, Ce anomalies can also be produced by bio-mediated reactions in anoxic environments (Kraemer and Bau, 2022).

Here we propose to use stable Ce isotopes to constrain the processes and the reaction rates responsible for the Ce behaviour in natural environments. Cerium has four stable isotopes of masses 136 (0.19 %), 138 (0.25 %), 140 (88.41 %) and 142 (11.15 %). The Ce isotopic composition is reported as the per mil variation from the Ce isotope standard LMV using the equation:

$$\delta^{142}Ce = \left(\frac{^{142}Ce/^{140}Ce_{sample}}{^{142}Ce/^{140}Ce_{LMV}} - 1 \right) \times 1000 \qquad \text{Eq. 1}$$

We developed a triple spike method for measuring mass-dependent fractionation of Ce isotopes (Bonnand et al., 2019). Cerium isotope variations in absorption experiments have also been performed (e.g., Nakada et al., 2013a). It has been shown that Ce isotopes are fractionated during Mn-Fe oxyhydroxide precipitation, with the precipitates enriched in light Ce isotopes. Natural samples have also been measured and ferromanganese nodules are a potential target to study redox changes in the palaeo-oceans (Nakada et al., 2016). It has been proposed that aqueous speciation is the main factor controlling Ce isotope fractionation (Nakada et al., 2017). To date, there is no investigation of the Ce isotopic fractionation during the Ce^{3+} to Ce^{4+} oxidation reaction. Accordingly, we performed two series of oxidation experiments to quantify the isotopic fractionation produced during the Ce^{3+} oxidation reaction, as well as measured the isotopic compositions of sediment samples characterised by different elemental cerium anomalies.

Results

The Ce concentration and isotopic composition of the oxidation experiments are presented in Table S-1. We performed two sets of experiments with varying oxidation duration (set 1, 3 minutes oxidation; set 2, 20 minutes). The Ce^{3+} was oxidised at room temperature, with varying amounts of a strong oxidising agent ($NaBrO_3$ + 10 M HNO_3). Varying the amount of oxidising agent enables partial oxidisation experiments with both Ce^{3+} and Ce^{4+} in solution (see Supplementary Information for details). The Ce^{3+} and Ce^{4+} fractions were chemically separated using ion-exchange chromatography (see Supplementary Information for details). In both sets of experiments, the amount of Ce^{3+} decreased from 3000 ng to 0 ng when oxidation proceeded, which translates to Ce/Ce* anomalies up to 0.1 as approximated by the Ce^{4+}/Ce_{TOT} ratio. The Ce^{3+} and Ce^{4+} fractions were analysed for their Ce isotopic composition. In the set 1 experiment (3 minutes), the Ce^{3+} fraction became isotopically heavy while oxidation proceeded. The Ce isotopic compositions varied from 0 ‰ to +0.4 ‰. The Ce^{4+} fraction was isotopically lighter than the Ce^{3+} fraction and became heavier while oxidation proceeded (Fig. 1a). In the 20 minutes experiments, the isotopic
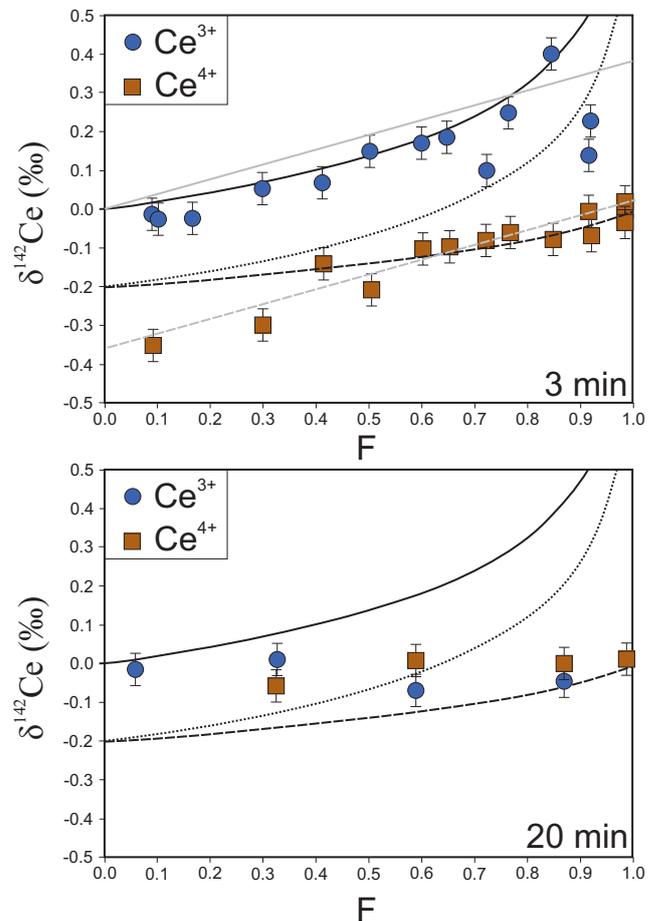
Figure 1 Ce isotopic composition for the Ce^{3+} and Ce^{4+} fractions in the oxidation experiments performed in this study. F is the fraction of Ce^{4+} produced during the reaction. The full, dotted and dashed lines are the Rayleigh fractionation models for the residual Ce^{3+}, the instantaneous Ce^{4+} and cumulated Ce^{4+}, respectively. The full and dashed grey lines are for the equilibrium model for the Ce^{3+} and Ce^{4+}, respectively. See text for details.

composition of the Ce^{3+} fraction was within error of the Ce^{4+} fraction (Fig. 1b) and very close to 0 ‰.

We have also analysed natural samples to determine whether samples with Ce elemental anomalies associated with redox reactions have a different isotopic composition compared to samples with Ce anomalies due to REE addition during alteration. The external reproducibility of our analytical technique has been determined by multiple measurements of two geological reference materials. To this end, BHVO-2 and GSP-2 were measured several times and we obtained $\delta^{142}Ce$ values of 0.087 ± 0.045 ‰ (n = 4) and 0.045 ± 0.044 ‰ (n = 4). Similarly, all geological samples (igneous and sedimentary rocks) analysed by Pourkhorsandi et al. (2021) have Ce isotopic compositions slightly heavier than their Ce standard. The Ce isotopic composition of natural samples analysed in this study are presented in Table S-2 and Figure 2. Analysed carbonate samples come from different locations (see Supplementary Information for details). They show the largest variations in $\delta^{142}Ce$ values (from 0.081 ‰ to 0.280 ‰). Banded iron formation (BIF) samples from the 3.22 Ga Moodies Group, Barberton Greenstone Belt, South Africa, have $\delta^{142}Ce$ values ranging from −0.055 ‰ to −0.007 ‰. Finally, two USGS Mn nodules (NOD-A1 and NOD-P1) are characterised by $\delta^{142}Ce$ values of 0.116 ‰ and 0.142 ‰, respectively. The carbonate samples show a covariation between Ce isotopic compositions and Ce elemental anomalies (Fig. 2).
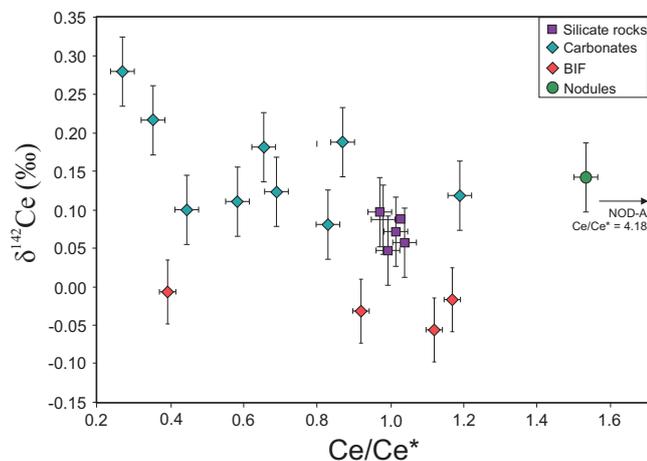
Figure 2 Ce isotopic compositions *versus* elemental cerium anomaly in the studied samples. The Ce anomaly is calculated using geometric extrapolation (see Barrat *et al.*, 2022) and the equation Ce/Ce* = Ce/(Pr^2/Nd) from Lawrence *et al.* (2006). See Table S-3 for details.

Discussion

We measured Ce isotope fractionations during oxidation of Ce^{3+} in two series of laboratory experiments, one lasting 3 minutes and one lasting 20 minutes. We observed that the amount of Ce^{4+} produced during the oxidation experiments was not dependent on the duration of the experiments but was strongly correlated to the amount of oxidising agent added to the original Ce^{3+}. As oxidation proceeded and the Ce^{3+} concentrations decreased, δ^{142}Ce values of the remaining unoxidised Ce^{3+} increased, indicating preferential oxidation of the lighter isotopes (Fig. 1). The isotopic composition of the Ce^{4+} produced during the reaction is isotopically light and varies from −0.32 ‰ to +0.08 ‰. The observed variations in δ^{142}Ce, presented in Figure 1, could be explained by either a Rayleigh fractionation or an equilibrium fractionation model. As illustrated in Figure 1, the isotopic fractionation factor ($\alpha_{Ce3+-Ce4+}$) obtained for the experiments using a Rayleigh fractionation model is 1.0002. The fractionation factor obtained with an equilibrium fractionation model is 1.00035. Given the fact that the reaction is unidirectional, we prefer the Rayleigh fractionation model for explaining the observed variations. As shown in Figure 1, the Ce isotopic composition for the Ce^{4+} fractions at low degree of partial oxidation is not perfectly aligned with the Rayleigh fractionation model. This variability could be explained by two hypotheses: 1) the small amount of Ce^{3+} left in solution tends to re-equilibrate faster than at lower oxidation reaction rate; or 2) during the chemical separation of Ce^{3+} and Ce^{4+} fractions, there was isotopic fractionation occurring that could not be corrected using the triple spike technique. Nevertheless, the isotopic effect during oxidation reactions is clearly demonstrated in Figure 1. The isotopic variations observed after 20 minutes are different from those of the 3 minute experiments. Ce^{3+} and Ce^{4+} fractions have similar isotopic compositions after 20 minutes. This suggests that Ce^{3+} and Ce^{4+} had enough time to re-equilibrate in the solutions. It also implies that, at equilibrium, there is no isotopic difference between Ce^{3+} and Ce^{4+} in our medium. Importantly, the fractionation factors obtained for our experiments are similar to those of absorption experiments on Mn oxides (Nakada *et al.*, 2013b) which suggests that oxidation of Ce^{3+} is one of the main mechanisms responsible for Ce isotopic variations in natural aquifers. The obtained fractionation factors should be applicable to aquifers where abiotic Ce oxidation dominates.

Cerium isotopes are fractionated during oxidation reactions and it follows that, in natural environments, this process occurs. The Ce^{4+} is isotopically light and the Ce^{3+} remaining in solution is isotopically heavier. In natural waters, Ce^{4+} being insoluble is readily removed. It follows that the remaining Ce in solution will become progressively heavy during this process. It also suggests that precipitates of Ce^{4+} should be isotopically light compared to the initial isotopic composition. It should be noted that the 20 minute experiments show that, at equilibrium, there is no isotopic fractionation between Ce^{3+} and Ce^{4+} in solution. In order to preserve the oxidation reaction signature in natural environments, it is thus important that the Ce^{4+} fraction is readily removed from the system. Although seawater samples have not been measured yet, and isotopic variations observed in our experiments may not be directly applicable to natural environments, we speculate that, because of oxidation reactions and subsequent removal of isotopically light Ce^{4+}, seawater should be isotopically heavy compared to the continental crust. This, of course, is variable in time, and stable Ce isotope variations in ancient sediments could be a powerful tool to study oxidation of past oceans and the rise of oxygen in the atmosphere.

In order to quantify the variability of Ce isotopic compositions in natural systems, a number of natural samples have been measured (eight carbonates, four banded iron formations and two Mn nodules). The carbonate samples analysed span a large range of elemental Ce anomalies (0.24 to 1.08) and are characterised by variable Ce isotopic compositions. As illustrated in Figure 2, there is a covariation between elemental Ce anomaly and mass dependent Ce isotopic composition in the analysed carbonates. It is widely accepted that negative Ce anomalies in sediments are interpreted as reflecting oxic conditions. The negative co-variation between Ce/Ce* and δ^{142}Ce in carbonates indicates that the Ce anomaly is, indeed, associated with redox reactions. As Ce/Ce* decreases, the Ce isotopic composition becomes heavier, which is consistent with oxidation reactions driving the appearance of the negative Ce anomaly.

Four banded iron formations from the 3.22 Ga Moodies Group (Barbeton Greenstone Belt, South Africa) have been analysed for their Ce isotopic composition. The BIF samples were also characterised by large negative elemental Ce anomalies. Amongst BIF samples, however, no Ce isotopic variations are observed. This suggests that the production of negative Ce anomaly is not linked to redox reactions. The Ce anomalies in the Moodies BIF analysed in this study have previously been linked to a late fluid circulation event not related to the conditions during deposition of these chemical sediments (Bonnand *et al.*, 2020). The results obtained in this study agree with this finding. In details, the Ce isotopic compositions in the BIF samples analysed in this study are slightly negative compared to the continental crust value. This result could be interpreted to reflect the incorporation of isotopically light Ce^{4+} into the BIF lattice. Although this hypothesis should be confirmed with further studies, it clearly highlights the complementarity between elemental Ce anomaly and the Ce isotopic composition to track the presence of atmospheric oxygen in marine chemical archives such as BIFs or carbonates.

Finally, the two analysed Mn nodules are characterised by large elemental positive Ce anomalies (1.39 and 3.78; Table S-2). Their Ce isotopic compositions are amongst the heaviest samples analysed in this study. Although the source of Ce in Mn nodules can be heterogenous (*e.g.*, seawater, hydrothermal and pore fluids), it suggests that these samples do record redox reactions within the Ce cycle in the Ocean and this result agrees with previously published results on ferromanganese deposits (Nakada *et al.*, 2016). Fe-Mn oxyhydroxides actively oxidise Ce by surface precipitation which suggests that the Ce incorporated in the Mn nodules can come from isotopically fractionated

seawater. It is likely that the ambient seawater was isotopically heavier than the Ce isotopic composition recorded in these samples (Nakada *et al.*, 2013b). It is also important to note that the analysed nodules are mixed-type nodules and Ce isotopes may also record secondary processes, such as diagenetic reactions.

Conclusions

The results presented here demonstrate that Ce isotopes are a powerful redox proxy for past and present environments. The co-variations between Ce anomaly and stable Ce isotopic composition indicate that Ce isotopes can be used to demonstrate the nature of Ce elemental anomalies. It will allow the distinction between redox driven Ce anomaly and elemental anomalies driven by secondary processes not related to redox conditions. It could also be useful to distinguish between Ce anomalies produced with and without the presence of oxygen. Mass dependent Ce isotope variations can also be coupled to radiogenic Ce. Using the La-Ce systematics, the La fractionation from Ce in old sediments can be dated which means that Ce anomaly and mass dependent Ce isotope variations are some of the few redox proxies that can be directly dated, providing exceptional insights into the early Earth oxygenation history.

Acknowledgements

Editor: Claudine Stirling

Additional Information

Supplementary Information accompanies this letter at https://www.geochemicalperspectivesletters.org/article2340.

References

Barrat, J.-A., Bayon, G., Lalonde, S. (2022) Calculation of cerium and lanthanum anomalies in geological and environmental samples. *Chemical Geology* 615, 121202. https://doi.org/10.1016/j.chemgeo.2022.121202

Bau, M., Koschinsky, A. (2009) Oxidative scavenging of cerium on hydrous Fe oxide: Evidence from the distribution of rare earth elements and yttrium between Fe oxides and Mn oxides in hydrogenetic ferromanganese crusts. *Geochemical Journal* 43, 37–47. https://doi.org/10.2343/geochemj.1.0005

Bau, M., Schmidt, K., Koschinsky, A., Hein, J., Kuhn, T., Usui, A. (2014) Discriminating between different genetic types of marine ferro-manganese crusts and nodules based on rare earth elements and yttrium. *Chemical Geology* 381, 1–9. https://doi.org/10.1016/j.chemgeo.2014.05.004

Bonnand, P., Israel, C., Boyet, M., Doucelance, R., Auclair, D. (2019) Radiogenic and stable Ce isotope measurements by thermal ionisation mass spectrometry. *Journal of Analytical Atomic Spectrometry* 34, 504–516. https://doi.org/10.1039/C8JA00362A

Bonnand, P., Lalonde, S.V., Boyet, M., Heubeck, C., Homann, M., Nonnotte, P., Foster, I., Konhauser, K.O., Köhler, I. (2020) Post-depositional REE mobility in a Paleoarchean banded iron formation revealed by La-Ce geochronology: A cautionary tale for signals of ancient oxygenation. *Earth and Planetary Science Letters* 547, 116452. https://doi.org/10.1016/j.epsl.2020.116452

Brumsack, H.-J. (2006) The trace metal content of recent organic carbon-rich sediments: Implications for Cretaceous black shale formation. *Palaeogeography, Palaeoclimatology, Palaeoecology* 232, 344–361. https://doi.org/10.1016/j.palaeo.2005.05.011

Eickmann, B., Hofmann, A., Wille, M., Bui, T.H., Wing, B.A., Schoenberg, R. (2018) Isotopic evidence for oxygenated Mesoarchaean shallow oceans. *Nature Geoscience* 11, 133–138. https://doi.org/10.1038/s41561-017-0036-x

Elderfield, H., Upstill-Goddard, R., Sholkovitz, E.R. (1990) The rare earth elements in rivers, estuaries, and coastal seas and their significance to the composition of ocean waters. *Geochimica et Cosmochimica Acta* 54, 971–991. https://doi.org/10.1016/0016-7037(90)90432-K

Farquhar, J., Bao, H., Thiemens, M. (2000) Atmospheric Influence of Earth's Earliest Sulfur Cycle. *Science* 289, 756–758. https://doi.org/10.1126/science.289.5480.756

German, C.R., Elderfield, H. (1990) Application of the Ce anomaly as a paleoredox indicator: The ground rules. *Paleoceanography* 5, 823–833. https://doi.org/10.1029/PA005i005p00823

Jenkyns, H.C. (2010) Geochemistry of oceanic anoxic events. *Geochemistry, Geophysics, Geosystems* 11, Q03004. https://doi.org/10.1029/2009GC002788

Kraemer, D., Bau, M. (2022) Siderophores and the formation of cerium anomalies in anoxic environments. *Geochemical Perspectives Letters* 22, 50–55. https://doi.org/10.7185/geochemlet.2227

Lawrence, M.G., Jupiter, S.D., Kamber, B.S. (2006) Aquatic geochemistry of the rare earth elements and yttrium in the Pioneer River catchment, Australia. *Marine and Freshwater Research* 57, 725–736. https://doi.org/10.1071/MF05229

Nakada, R., Takahashi, Y., Tanimizu, M. (2013a) Isotopic and speciation study on cerium during its solid-water distribution with implication for Ce stable isotope as a paleo-redox proxy. *Geochimica et Cosmochimica Acta* 103, 49–62. https://doi.org/10.1016/j.gca.2012.10.045

Nakada, R., Tanimizu, M., Takahashi, Y. (2013b) Difference in the stable isotopic fractionations of Ce, Nd, and Sm during adsorption on iron and manganese oxides and its interpretation based on their local structures. *Geochimica et Cosmochimica Acta* 121, 105–119. https://doi.org/10.1016/j.gca.2013.07.014

Nakada, R., Takahashi, Y., Tanimizu, M. (2016) Cerium stable isotope ratios in ferromanganese deposits and their potential as a paleo-redox proxy. *Geochimica et Cosmochimica Acta* 181, 89–100. https://doi.org/10.1016/j.gca.2016.02.025

Nakada, R., Tanaka, M., Tanimizu, M., Takahashi, Y. (2017) Aqueous speciation is likely to control the stable isotopic fractionation of cerium at varying pH. *Geochimica et Cosmochimica Acta* 218, 273–290. https://doi.org/10.1016/j.gca.2017.09.019

Ohta, A., Kawabe, I. (2001) REE(III) adsorption onto Mn dioxide (δ-MnO_2) and Fe oxyhydroxide: Ce(III) oxidation by δ-MnO_2. *Geochimica et Cosmochimica Acta* 65, 695–703. https://doi.org/10.1016/S0016-7037(00)00578-0

Pourkhorsandi, H., Debaille, V., de Jong, J., Armytage, R.M.G. (2021) Cerium stable isotope analysis of synthetic and terrestrial rock reference materials by MC-ICPMS. *Talanta* 224, 121877. https://doi.org/10.1016/j.talanta.2020.121877

Reinhard, C.T., Planavsky, N.J. (2022) The History of Ocean Oxygenation. *Annual Review of Marine Science* 14, 331–353. https://doi.org/10.1146/annurev-marine-031721-104005

Tostevin, R., Shields, G.A., Tarbuck, G.M., He, T., Clarkson, M.O., Wood, R.A. (2016) Effective use of cerium anomalies as a redox proxy in carbonate-dominated marine settings. *Chemical Geology* 438, 146–162. https://doi.org/10.1016/j.chemgeo.2016.06.027